ORIGINAL PAPER

Scanning reflectance spectroscopy (380–730 nm): a novel method for quantitative high-resolution climate reconstructions from minerogenic lake sediments

M. Trachsel · M. Grosjean · D. Schnyder ·
C. Kamenik · B. Rein

Abstract High-resolution (annual to sub-decadal) quantitative reconstructions of climate variables are needed from a variety of paleoclimate archives across the world to place current climate change in the context of long-term natural climate variability. Rapid, high-resolution, non-destructive scanning techniques are required to produce such high-resolution records from lake sediments. In this study we explored the potential of scanning reflectance spectroscopy (VIS-RS; 380–730 nm) to produce quantitative summer temperature reconstructions from minerogenic sediments of proglacial, annually laminated Lake Silvaplana, in the eastern Swiss Alps. The scanning resolution was 2 mm, which corresponded to sediment deposition over 1–2 years. We found correlations up to $r = 0.84$ ($p < 0.05$) for the calibration period 1864–1950, between six reflectance-dependent variables and summer (JJAS) temperature. These reflectance-dependent variables (e.g. slope of the reflectance 570/630 nm, indicative of illite, biotite and chlorite; minimum reflectance at 690 nm indicative of chlorite) indicate the mineralogical composition of the clastic sediments, which is, in turn, related to climate in the catchment of this particular proglacial lake. We used multiple linear regression (MLR) to establish a calibration model that explains 84% of the variance of summer (JJAS) temperature during the calibration period 1864–1950. We then applied the calibration model downcore to develop a quantitative summer temperature reconstruction extending back to AD 1177. This temperature reconstruction is in good agreement with two independent temperature reconstructions based on documentary data that extend back to AD 1500 and tree ring data that extend back to AD 1177. This study confirms the great potential of in situ scanning reflectance spectroscopy as a novel non-destructive technique to rapidly acquire high-resolution quantitative paleoclimate information from minerogenic lake sediments.

M. Trachsel (✉) · M. Grosjean · D. Schnyder ·
C. Kamenik
Department of Geography, University of Bern,
Erlachstrasse 9a, 3012 Bern, Switzerland
e-mail: trachsel@giub.unibe.ch

M. Trachsel · M. Grosjean · C. Kamenik
Oeschger Centre for Climate Change Research,
University of Bern, Zähringerstrasse 25, 3012 Bern,
Switzerland

B. Rein
Institute for Geosciences, University of Mainz,
Becherweg 21, 55099 Mainz, Germany

B. Rein
GeoConsult Rein, Gartenstrasse 26-28, 55276
Oppenheim, Germany

Introduction

High-resolution, well calibrated temperature reconstructions are fundamental to put current warming into a longer-term perspective. To improve knowledge of past climate and further constrain uncertainties in climate reconstructions, new high-quality time series of proxy climate data are required. These proxy series must fulfill several criteria that are fundamental for quantitative reconstructions: (1) the proxy data must be highly correlated with climate variables, (2) data must be collected at high temporal resolution (i.e. annual to multi-year intervals), and (3) the record must be precisely dated.

In the past decade, considerable advances have been made in the use of geochemical proxies in lake sediments for reconstructing past climate. These reconstructions were based on sedimentological or geochemical analysis of thin sections (Francus et al. 2002; Kalugin et al. 2007) or sediment subsamples (McKay et al. 2008; Kaufman et al. 2009). Such analyses were destructive and required time-consuming sample preparation. Major developments have also taken place in the exploration of methods of direct measurement on sediment cores using non-destructive scanning techniques such as X-ray fluorescence (Zolitschka et al. 2001).

Little, however, has been done on scanning reflectance spectroscopy in the visible spectrum (VIS-RS; 380–730 nm), another non-destructive rapid scanning method (Rein and Sirocko 2002). One advantage of this method is that data acquisition is rapid and inexpensive. Several meters of sediment core can be processed at 2-mm measuring intervals in a day (i.e. >1,000 data points can be generated), and the same sediment can be used for further analyses. More difficult are data analysis, interpretation, and transformation of raw reflectance spectroscopy data into quantitative variables that represent specific sediment compounds, and ultimately are informative about climate or environmental change. Reflectance spectroscopy in the visible and infrared range is widely used to detect organic components in lake sediments (Rosen et al. 2000; Rein and Sirocko 2002; Wolfe et al. 2006; Michelutti et al. 2009). However, non-destructive scanning reflectance spectroscopy, with direct in situ measurement of split sediment cores is far less common. This method has been used to detect organic and clastic components in marine

sediments off the coast of Peru (Rein and Sirocko 2002; Rein et al. 2005). In a recent study, von Gunten et al. (2009) used this scanning technique on biogenic freshwater sediments in eutrophic Laguna Aculeo, central Chile, to determine photopigments and produce high-resolution quantitative reconstructions of austral summer (DJF) temperatures.

In this study we explored the potential for applying this method to minerogenic freshwater sediments in a proglacial lake environment. We chose Lake Silvaplana, eastern Swiss Alps, for this methodological case study because the mineralogical and geochemical composition of the sediment is well known from established analytical techniques (X-ray diffraction, ICP-OES measurements of biogenic Si, grain size distributions and Mass Accumulation Rate (Blass et al. 2007a, b and references therein), and the mineralogical composition of individual varves has been shown to be controlled by climate (Trachsel et al. 2008). These sediments contain <1% organic material. The rest is composed of mineroclastic fine silt particles that are transported as suspended load from glacial meltwater and rainfall runoff (Blass et al. 2007a).

The overall goals of this study were: (1) to systematically test the method and the significance of the data produced, and (2) to describe how raw reflectance measurements can be used to make quantitative climate reconstructions. We use published algorithms that describe the reflectance characteristics of minerals identified in the sediments of Lake Silvaplana using XRD. In addition, we present further algorithms that describe the remaining, as yet unexplained distinct characteristics of the measured sediment reflectance spectra. Each of these algorithms is then used to produce a spectrum-derived variable. To gain further insight into the 'known' and 'unknown' variables extracted, we applied a Principal Component Analysis (PCA) to the variables to detect similarities. Subsequently, we transformed the raw reflectance data (variables) into a climate reconstruction, which involved four steps: (1) testing the effects of climate variables and sediment parameters on the spectrum-derived variables, using redundancy analysis RDA, (2) establishing univariate and multivariate calibration models for climate and sediment parameters, (3) applying the optimal calibration model downcore (reconstruction), and (4) verifying the reconstruction back in time to AD 1177, with fully independent data sets.

Study site

Lake Silvaplana (Lej da Silvaplauna, Fig. 1, 46°27′N, 9°48′E) is a postglacial, high-elevation (1,800 m), 2.7-km^2 (water volume 127×10^6 m^3), 77-m deep, dimictic lake of glacio-tectonic origin. The lake is typically ice-covered between January and May. The catchment is 129 km^2 and reaches an elevation of 3,441 m. About 6 km^2, 5% of the catchment, were glaciated in 1998. The Fedacla River, with average runoff 1.5 m^3 s^{-1}, is the only glacial river in the catchment and, therefore, the principle conveyor of sediments to the lake. The Inn River, connecting Lake Sils with Lake Silvaplana, is larger (discharge 2 m^3 s^{-1}), but is almost devoid of sediments. Two small rivers (Vallun; 0.7 m^3 s^{-1} and Surlej; 0.3 m^3 s^{-1}) are particularly active during spring snowmelt and summer rainstorms.

The specific geological setting of the basin was fundamental to our study. Lake Silvaplana is located on the tectonic Engadine Line, which separates the Lower Austroalpine basement (granites with high

Fig. 1 Overview map of the Lake Silvaplana catchment area, including the coring location, meteorological station, geology and the glacier extent during the Little Ice Age and in 1991 (redrawn from Blass et al. 2007a)
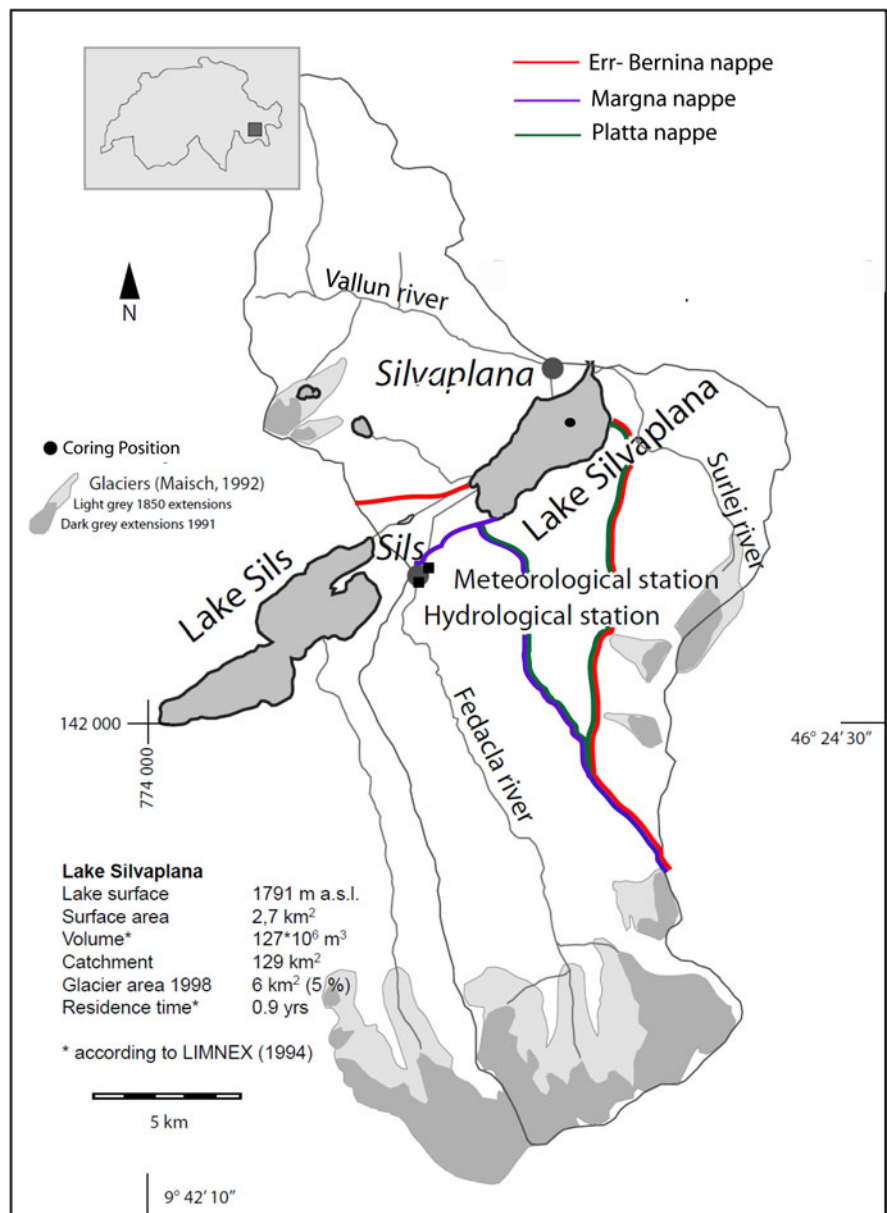
amounts of feldspar, Err-Bernina nappe) in the northwest and east from the Penninic basement (orthogneiss and gabbro, with high amounts of mica, Margna nappe and Platta nappe, Fig. 1) in the south (Spillmann 1993). These spatial differences in geology are apparent in the mineral spectra of sediments around the shore of the lake (Ohlendorf 1998).

The Engadine exhibits climate typical for an inner-Alpine dry valley. Maximum monthly precipitation occurs in August (121 mm), whereas a minimum is observed in February (42 mm). Annual precipitation amounts to 978 mm (1961–1990, SMA 2002). Mean monthly temperature ranges from $-7.2°C$ (January) to $10.4°C$ (July).

Materials and methods

A gravity core (SVP 06-1) and two piston cores (06-2 and 06-3) were collected from Lake Silvaplana in March 2006. The chronology of the top section (SVP 06-1; AD 1620 onwards) was established by visual correlation of 16 diagnostic sediment strata (nine flood layers for the calibration period 1864–1950; seven flood layers 1620–1864) with the master chronology developed for freeze cores in previous work by varve counting and documented flood layer events (Blass et al. 2007a; Trachsel et al. 2010) and interpolated with a mixed-effect regression model (Heegaard et al. 2005). Maximum error in the chronology was ±7 years. The chronology of cores SVP 06-2 and SVP 06-3 (AD 1177–1620) was established using varve counts and historically documented flood layer events (Caviezel 2007), extending the record back to AD 1177 (Trachsel et al. 2010).

For numerical calibration analysis we used the data set from the time period 1864–1950 for which monthly temperature and precipitation data are available from the nearby Sils–Maria meteorological station (Begert et al. 2005). After 1950, anthropogenic eutrophication (Blass et al. 2007b; Bigler et al. 2007) strongly affected sediment composition, which in turn affects the reflectance characteristics of the sediment and masks the climate signal (Rein and Sirocko 2002; Wolfe et al. 2006).

The reflectance data were acquired by high-resolution photospectrometric logging of split cores with a Gretag Spectrolino (GretagMacbeth, Switzerland). The aperture of the sensor is 2.5 mm and the

spectral coverage ranges from 380 to 730 nm, with a spectral resolution of 3 nm integrated into bands of 10-nm intervals. The photo-spectrometer uses a ceramic plate (BCA–GretagMacbeth) as a white standard. Prior to analysis the split cores were covered with polyethylene transparent foil to minimise oxidation and avoid contamination of the sensor head. Wavelength-dependent illumination and transparency effects were corrected by dividing each spectrum acquired from the sediment by that of the transparency-covered standard (Rein and Sirocko 2002). The measurement interval on the core was 2 mm.

After data acquisition, diagnostic reflectance characteristics, hereafter referred to as 'variables,' were extracted from the overall reflectance spectra by applying specific algorithms (Rein and Sirocko 2002; Wolfe et al. 2006). In Lake Silvaplana the reflectance spectra are combinations of the reflectance spectra of the main minerals present in the sediment, i.e. quartz, mica (muscovite, biotite, illite), chlorite, plagioclase and amphibole (Ohlendorf 1998; Trachsel et al. 2008).

For this study, we used four algorithms that are well established and documented in the literature and are indicative of illite, biotite and chlorite (Rein 2003; USGS 2007), and two algorithms that describe further characteristics of the spectra but are presently 'unknown' (Table 1). In general, either slopes of reflectance spectra in defined windows (Rein and Sirocko 2002; Wolfe et al. 2006), relative absorption band depths (Rein and Sirocko, 2002), or relative absorption band areas (Rein and Sirocko 2002; Wolfe et al. 2006) were used to describe the spectra (Fig. 2b).

In general, a relative absorption band depth (RABD, min) is defined as the ratio between the value measured in a reflectance minimum and the value obtained for the same wavelength, assuming a linearly interpolated reflectance continuum (blue line, Fig. 2b) between two maxima (Fig. 2b). Hence, it is the ratio between the points denoted with a and b in Fig. 2b.

Point a can be obtained by distance weighting of the maxima, i.e.

$$a = \frac{(x3 - x2) \cdot y1 + (x2 - x1) * y3}{(x3 - x1)},$$

or by adding the slope multiplied with the distance, to one maximum:

Table 1 Algorithms for the calculation of the six VIS-RS-derived variables

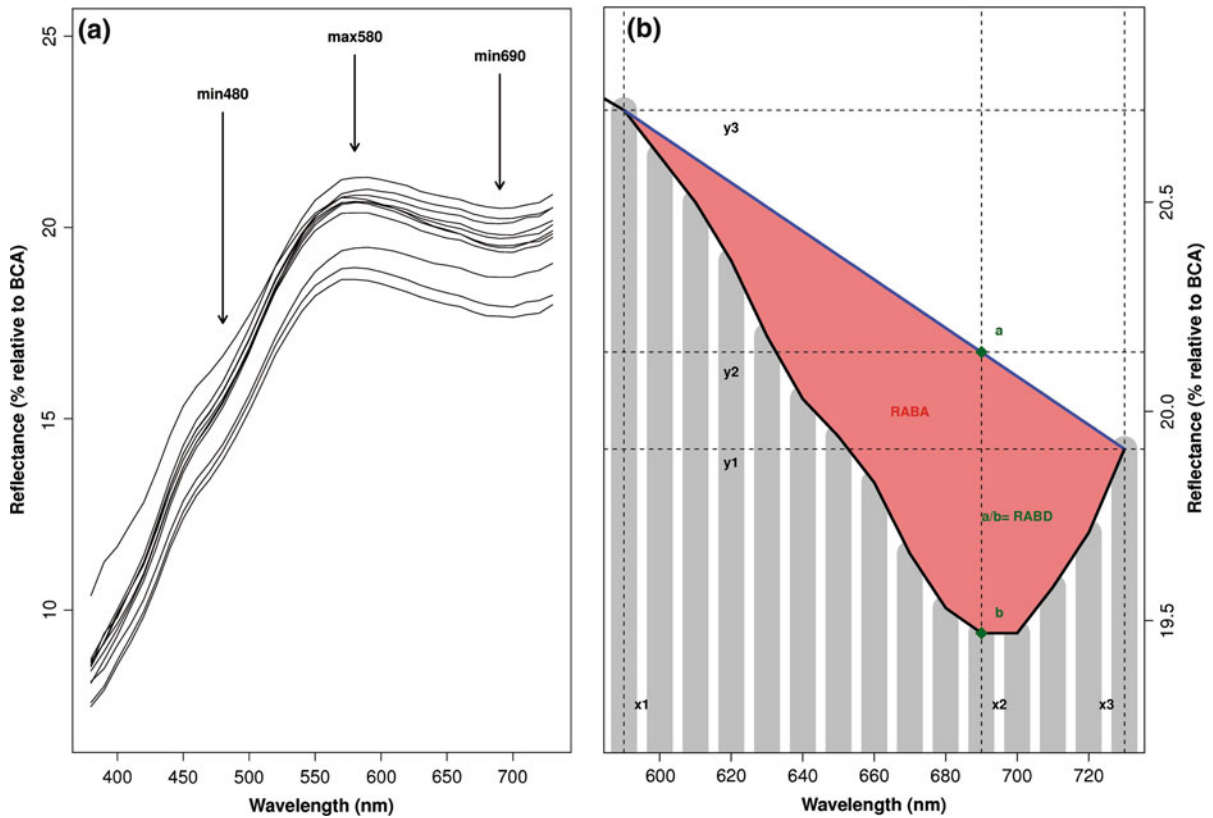| Algorithm		
$R_{590}dR_{690}$	R_{590}/R_{690}	Biotite, Illite, Chlorite (USGS 2007)
$R_{570}dR_{630}$	R_{570}/R_{630}	Biotite, Illite, Chlorite (Rein 2003)
Min_{690}	$[(4*R_{590} + 10*R_{730})/14]/R_{690}$	Chlorite (USGS 2007)
$Trough_{590-730}$	$(141*R_{730} + [141*(R_{590} - R_{730})/2] - (6*R_{590} + 5*R_{730}) - 10*\sum R_{600-720})/Rmean$	Chlorite (USGS 2007)
$Min_{690}or_{700}$	$[(R_{660} + 3*R_{710})/4]/R_{690}or_{700}$	Unknown
Min_{480}	$[(R_{460} + 2*R_{490})/3]/R_{480}$	Unknown

Fig. 2 a Selected reflectance spectra of the clastic sediment (prior to 1950) of Lake Silvaplana and **b** illustration for calculating variables. The figure shows measured reflectance data (*black line*), linearly interpolated reflectance continuum between two maxima (*blue line*), points *a* and *b* used for calculating Relative Absorption Band Depth (RABD) and the area considered as Relative Absorption Band Area (*red*). BCA is the white standard based on barium sulfate

$$a = y1 + \frac{y3 - y1}{x3 - x1} * (x2 - x1)$$
$$= \frac{y1 \cdot (x3 - x1) + (y3 - y1) \cdot (x2 - x1)}{(x3 - x1)}$$

Elementary calculus proves the equality of these two approaches.

Relative absorption band area (RABA, trough) is defined by the area between the measured reflectance and the linearly interpolated reflectance between two maxima described above (red area in Fig. 2b), divided by the overall reflectance. This area is defined by the rectangle constrained by 0 and y1, and x1 and

x3 (area $= y1 \times (x3 - x1)$ plus the triangle between the points (x3, y1), (x1, y1), (x1, y3),

$$\left(\text{area} = \frac{(x3 - x1) * (y3 - y1)}{2} \right)$$

We then have to subtract the area below the measured reflectance curve (black curve, grey bars Fig. 2b). Because one measured value is covering a bandwidth of 10 nm, we have to subtract $10 * R_{(max1+10; \ i.e.600)} \ \dots \ 10 * R_{(max2-10 \ i.e. \ 720)}$ and half of the bands of the first (max1) and the second (max2) maximum, respectively, i.e. $6 * R_{(max1; \ i.e. \ 590)}$ and $5 * R_{(max2; \ i.e. \ 730)}$.

This results in the general formula:

$$\text{RABA} = (y1 * (x3 - x1) + \frac{(x3 - x1) * (y3 - y1)}{2}$$
$$- 10 * \sum R_{(max1+10)-(max2-10)} - 6 * R_{(max \ 1)}$$
$$- 5 * R_{(max \ 2)}) / R_{mean}$$

A comprehensive collection of reflectance spectra for different minerals can be found in the spectral library of the US Geological Survey (USGS 2007). Rein and Sirocko (2002) assigned the slope of the reflectance spectra of sediments between 570 and 630 nm to the amount of clastic material, i.e. the amount of illite or chlorite, in the sediment (Rein 2003). In Lake Silvaplana the spectra have a maximum at 580–590 nm and a minimum at 690–700 nm (Fig. 2a). The maximum at 590 nm can be assigned to the amount of illite, biotite (both mica) and chlorite; the minimum at 690 nm can be attributed to the amount of chlorite (USGS 2007). The presence and relative abundance of these minerals in the sediments of Lake Silvaplana has been experimentally documented by XRD analysis of more than 400 individual varves (Trachsel et al. 2008).

To link the amount of different minerals and the mineral composition in the sediments of Lake Silvaplana to local climate variables, we followed the model of Trachsel et al. (2008). Three different geological formations with diagnostic bedrock composition crop out in the catchment, which results in a different mineralogical composition of the sediment from different tributaries (Ohlendorf 1998). Because the bedrock geology of the glaciated part in the catchment is relatively enriched in mica (biotite, illite) and chlorite, the sediment transported by glacial meltwater during warm summers carries that

signature. The relative proportion of these minerals can be detected by XRD or by specific characteristics of the reflectance spectra.

Prior to numerical analysis, all turbidites were removed from the sediment record, and the raw reflectance data were converted into a time series with homogenous (annual) intervals using re-sampling and linear interpolation procedures. To account for the minimum instrumental sampling resolution and for dating uncertainties, we applied 5 and 9-year running means to the time series, referred to as 5- or 9-year smoothed.

Numerical methods, calibration and climate reconstruction

In this section we describe the numerical methods applied in this study. First we tested the independence of the reflectance-derived variables and assessed the amount of redundancy in the multivariate data set. In a second step we assessed the potential and suitability of reflectance-derived variables for climate reconstructions and calibrated the variables against local meteorological data. We compared univariate and multivariate calibration approaches since it was not known *a priori* whether an individual reflectance variable or a combination of variables reveals better calibration statistics.

The technical resolution, i.e. aperture of the Spectrolino instrument sensor is 2.5 mm. It is not known, however, if the technical resolution is equal to the area measured (2-mm increments) on the sediment core. To evaluate the effective measurement resolution and assess the independence of the individual measurements we calculated autocorrelations of the reflectance-derived variables for the calibration period 1864–1950. The significance of the lag-1 autocorrelations was tested with a *z*-test (Venables and Ripley 2002).

We then applied a Principal Component Analysis (PCA, Hotelling 1933) to our data to detect similarities among the six reflectance-dependent variables (Table 1; two variables for illite, biotite and chlorite, two for chlorite and two 'unknown') and tested the significance of the PC-axes with the broken stick model (Frontier 1976; Legendre and Legendre 1998). Blass et al. (2007a) and Trachsel et al. (2008) have shown that the amount of clastic material (i.e. the mass accumulation rate, MAR) and the mineralogical

composition of the sediment reflect summer temperature and summer precipitation. Therefore, we used redundancy analysis (RDA, van der Wollenberg 1977) to assess the sensitivity of the reflectance spectrum-derived variables to all possible combinations of the three variables 'MAR', 'temperature' and 'precipitation' for 5- and 9-year smoothed data (Table 3). The significance of RDA axes was assessed with permutation tests (Legendre and Legendre 1998). MAR shows a low-frequency trend related to glacier length fluctuations and is mainly influenced by summer temperatures on shorter (interannual, decadal to multi-decadal) timescales (Blass et al. 2007a). Therefore, in all cases where RDA reveals an influence of MAR on the reflectance-derived variables, we detrended our data set to remove effects that are related to the low-frequency trend in the MAR. We used locally weighted regression (loess, Cleveland and Devlin 1988) to detrend our data. The span of the filter was set to represent 100 years.

To detect relations between reflectance-derived variables and climate variables individually, we correlated unsmoothed, 5- and 9-year smoothed data with temperature and precipitation, using both raw data and loess detrended data. The degrees of freedom (DF) were corrected for autocorrelated time series according to Dawdy and Matalas (1964). Multiple testing was taken into account following Benjamini and Hochberg (1995). P values adjusted for autocorrelation are referred to as p_c, and p values adjusted for autocorrelation and multiple testing are referred to as p_{ca}.

To produce a summer temperature reconstruction, we used inverse regression to calibrate those VIS-RS variables individually that are significantly ($p_{ca} < 0.05$) correlated with detrended instrumental summer temperatures. We then tested whether multiple linear regression (MLR) yields better calibration models than univariate calibration. Leave–one-out cross-validated RMSEP was used to choose the best model (e.g. Kamenik et al. 2009). For the MLR model, we included an additional variable only if the RMSEP of the new model, with the additional variable, decreased by more than 5% (Birks 1998). Because the focus of this study was on the reflectance spectroscopy method, we did not compare the performance of MLR to other multivariate calibration approaches.

To assess the performance of our 800-year reflectance spectra-based summer temperature reconstruction, we compared our data with two independent reconstructions based on documentary and early instrumental data (Casty et al. 2005), and tree ring late-wood density data (Büntgen et al. 2006).

Results

Reflectance-derived variables, PCA

The reflectance spectra (Fig. 2a) of the sediments from Lake Silvaplana show distinct characteristics: a reflectance maximum at 580–590 nm is followed by decreasing reflectance with a minimum at 690–700 nm. The reflectance increases again towards 730 nm. A further local reflectance minimum is found at 480 nm. The six variables derived from the reflectance spectra and used in this study (Table 1) describe distinct characteristics of the spectra.

The time series of these six variables are shown in Fig. 3a–f. Three of them (Ratio $R_{590}dR_{690}$, Ratio $R_{570}dR_{630}$ and min480; Fig. 3d–f) exhibit a long-term trend, whereas no trend is detected for the other variables (Fig. 3a–c).

The lag-1 autocorrelation of the spectrum-derived time series during the calibration period is significant ($p < 0.05$) for all unsmoothed non-detrended data series as well as for unsmoothed detrended time series except for min_{480}. After 5- and 9-year smoothing, the lag-1 autocorrelation is higher than 0.9 for all variables. When smoothing with filters higher than 9-year, smoothing no longer increases the lag-1 autocorrelation.

The results for the PCA are shown in Table 2. For raw unsmoothed data, we found two significant PC-Axes, which explain 47 and 30% of the variance. The variables $R_{590}dR_{690}$, $R_{570}dR_{630}$, both indicative of illite, biotite (mica) and chlorite, the trough$_{590-730}$ and min_{690}, both indicative of chlorite, have high positive loadings in the first principal component PC1. PC2 loadings are positive for $R_{590}dR_{690}$ and $R_{570}dR_{630}$ (illite, biotite), but negative for trough$_{590-730}$ and min_{690} (chlorite). $Min_{690or700}$ and min_{480} have moderate negative loadings in PC1. $Min_{690or700}$ has a high negative loading in PC2, whereas the loading of min_{480} is moderately positive in PC2.

For the PCA of detrended spectrum-derived variables we find one significant PC which explains 54% of the variance. The relationship of the variables $R_{590}dR_{690}$, $R_{570}dR_{630}$, the trough$_{590-730}$ and min_{690} is
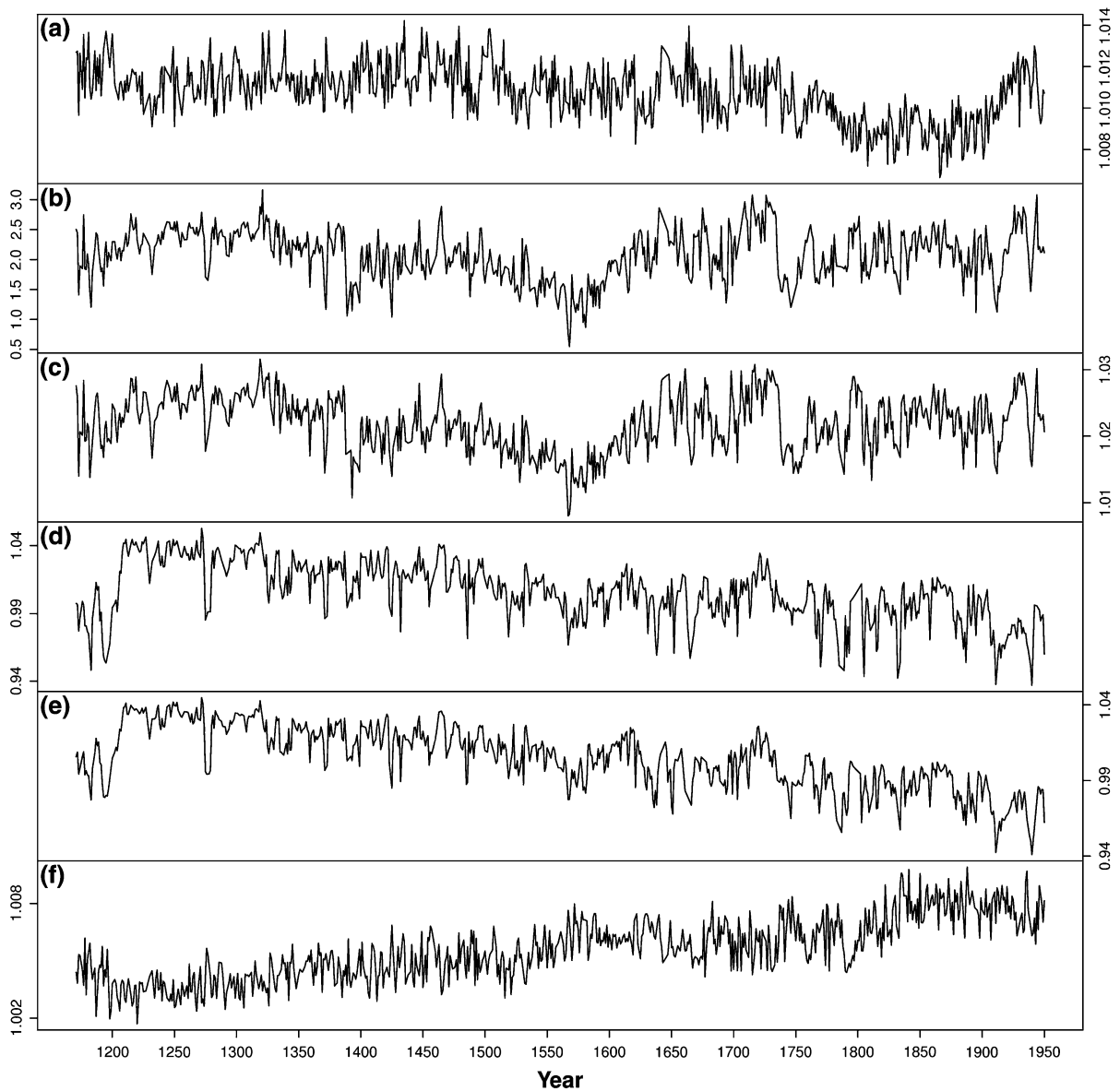
Fig. 3 Raw VIS-RS data time series for variables **a** $min_{690\ or\ 700}$, **b** $trough_{590-730}$, **c** min_{690}, **d** $R_{590}dR_{690}$, **e** $R_{570}dR_{630}$ and **f** min_{480}. *Note*: The *y*-axes in panels **a–f** are dimensionless because they represent reflectance ratios (see Table 1)

similar to the PCA for raw, non-detrended data (Table 2).

Calibration and climate reconstruction

After describing the data by PCA, we used RDA to look for environmental parameters that might influence the reflectance data. A series of RDA revealed highest influence of the summer season, temperature

(T) for months JJAS and precipitation (P) for months MJJAS.

For the raw reflectance data, T JJAS and MAR explain the highest proportion of variance, >25% for 5-year as well as for 9-year smoothed data (Table 3). The proportion of variance explained by P MJJAS is considerably lower and amounts to 8.5% for 5-year smoothed variables and to 16.3% for 9-year smoothed variables. Combined T JJAS and MAR

Table 2 Loadings of the VIS-RS-derived variables on the significant principal component axes for non-detrended and detrended VIS-RS data

Significant correlations ($p < 0.05$) between variables and axes are denoted with an *asterisk*

Non-detrended			Detrended	
Variable	Correlation with axis 1 = Loading	Correlation with axis 2 = Loading	Variable	Correlation with axis 1 = Loading
Min_{480}	−0.125	0.38*	Min480	0.19
$R_{590}dR_{690}$	0.88*	0.40*	$R_{590}dR_{690}$	0.85*
Min_{690}	0.84*	−0.46*	Min_{690}	0.93*
$Min_{690or700}$	−0.13	−0.92*	$Min_{690or700}$	0.29*
$R_{570}dR_{630}$	0.87*	0.42*	$R_{570}dR_{630}$	0.86*
$Trough_{590-730}$	0.77*	−0.53*	$Trough_{590-730}$	0.90*

Table 3 Amount of variation (%) explained by T JJAS, P MJJAS or MAR and their combinations among six VIS-RS-derived variables

		T JJAS	MAR	P MJJAS	T JJAS + MAR	T JJAS + P MJJAS	P MJJAS + MAR	T MJJAS + P MJJAS + MAR
Non-detrended data								
5-year VIS-RS data	1 RDA	25.7%*	22%*	8.5%*	26%* (24.3%*)	28.3%* (23.7%*)	23.4%* (3%*)	28.8%* (24.1%*)
	2 RDA (cum)				46%* (21.9%*)	32.2%* (6.9%*)	25.1%* (16.6%*)	49.1%* (2.8%*)
	3 RDA (cum)							49.2% (17%*)
9-year VIS-RS data	1 RDA	33.4%*	28%*	16.3%*	33.8%* (33.8%*)	33.7%* (29.4%*)	29.1%* (16.4%*)	33.9%* (30.6%*)
	2 RDA (cum)				61.6%* (28.25%*)	45.7% (12.29%*)	32.7% (16.4%*)	63.9%* (1.6%)
	3 RDA (cum)							64% (17.6%*)
Loess-detrended								
5-year VIS-RS data	1 RDA	29.4%*	5.5%*	6.9%*	29.5%* (25.3%*)	35.4%* (28.6%*)	9.9%* (5.3%*)	35.4%* (26.2%*)
	2 RDA (cum)				30.8% (1.4%)	35.5% (6%*)	10.8% (3.9%*)	37.5%* (6.2%*)
	3 RDA (cum)							37.6% (1.4%)
9-year VIS-RS data	1 RDA	44.8%*	9.3%*	12.2%*	44.9%* (37%*)	46.8%* (36.6%*)	17%* (8.4%*)	46.9%* (31.2%*)
	2 RDA (cum)				46.2% (1.4%)	46.9% (3.9%*)	17.6% (5.4%*)	48% (2.5%)
	3 RDA (cum)							48.5% (1.2%)

The values in parentheses are the unique values of the variables (order according to the headline). Significant RDA-axes ($p < 0.05$) and unique values of variables are denoted with an *asterisk*

explain more than 45% of the variance for 5-year as well as for 9-year smoothed data. Adding precipitation to T JJAS and MAR does not increase the proportion of explained variance. Thus, the third RDA axis is not significant. If only one explanatory variable is considered, i.e. excluding the effects of the other explanatory variables caused by multi-collinearity, T JJAS showed highest values.

For the detrended VIS-RS data sets, the variance explained by T JJAS was higher, compared with the raw data, whereas the variance explained by MAR and by P MJJAS was low. For the 5-year smoothed VIS-RS data, all of the three constraining data sets (temperature, precipitation and MAR) were significant ($p < 0.05$). The same was found for the 9-year smoothed VIS-RS data. When combining explanatory variables, only the first RDA-axis is significant ($p < 0.05$). The second and third RDA axes do not reach the significance level ($p < 0.05$) when the explanatory variables are

Table 4 Correlations between T JJAS and P MJJAS and spectrum-derived variables for (a) unsmoothed, 5- and 9-year smoothed data and (b) loess-detrended un-smoothed, 5- and 9-year smoothed spectrum-derived variables

	T JJAS			P MJJAS		
	Un-smoothed	5-year	9-year	Un-smoothed	5-year	9-year
Not detrended						
Min_{480}	−0.34**	−0.50	−0.58*	0.19	0.08	−0.04
$R_{590}dR_{690}$	0.23	0.60*	0.61	0.08	0.44	0.66*
Min_{690}	0.31*	0.70*	0.75*	−0.07	0.12	0.08
$Min_{690or700}$	0.05	0.00	0.07	−0.20	−0.25	−0.46
$R_{570}dR_{630}$	0.23	0.61*	0.60	0.09	0.39	0.56*
$Trough_{590-730}$	0.31*	0.73**	0.81*	−0.01	0.16	0.13
Detrended data						
Min_{480}	−0.31*	−0.51**	−0.63	0.13	−0.12	−0.36
$R_{590}dR_{690}$	0.26	0.72**	0.83**	0.04	0.38	0.50*
Min_{690}	0.26	0.66**	0.74	−0.07	0.21	0.26
$Min_{690or700}$	0.06	−0.01	0.00	−0.18	−0.08	−0.17
$R_{570}dR_{630}$	0.24	0.71**	0.84**	0.05	0.35	0.41
$Trough_{590-730}$	0.27	0.72**	0.82**	−0.07	0.20	0.32

* $p < 0.05$ taking into account autocorrelation

** $p < 0.05$ taking into account autocorrelation and multiple testing

combined. T JJAS again shows highest unique values.

Table 4 summarises the relationship between individual VIS-RS variables and climate variables. For raw (not detrended) reflectance data, the highest correlations are found between summer temperatures and the variables min_{690} and $trough_{590-730}$ (unsmoothed, 5- and 9-years). While the correlation of $trough_{590-730}$ with summer temperature fulfills the rigorous significance level for 5-year smoothed data ($p_{ca} < 0.05$ corrected for autocorrelation and multiple testing, marked with ** in Table 4), all other correlations are significant for $p_c < 0.05$ (marked with * in Table 4).

Reflectance variables are generally not significantly correlated ($p_c < 0.05$) with summer precipitation, except 9-year smoothed $R_{590}dR_{690}$ and $R_{570}dR_{630}$ (significant at $p_c < 0.05$).

For detrended data, the highest correlations with summer temperature are found for $R_{590}dR_{690}$, $R_{570}dR_{630}$ and $trough_{590-730}$. These correlations are significant ($p_{ca} < 0.05$) for 5-year and 9-year smoothed data series. For detrended precipitation, only one significant ($p_c < 0.05$) correlation was found after 9-year smoothing ($R_{590}dR_{690}$).

In summary, the variables $trough_{590-730}$, and to some extent $R_{590}dR_{690}$ and $R_{570}dR_{630}$, have the potential to serve as robust predictors for summer temperature. Although the variable $trough_{590-730}$ is also robust for raw (not detrended data), loess-detrending enhances the significance of the correlations with $R_{590}dR_{690}$ and $R_{570}dR_{630}$. As a result of the RDA and correlation analysis, a calibration for and reconstruction of 'precipitation' was rejected and no longer pursued.

Table 5 shows the quality of the calibration (criterion: leave-one-out RMSEP) between detrended reflectance data and summer temperatures for univariate and multivariate (2–6 variables) models. The multivariate calibration approaches yield consistently better results (smaller RMSEP) than models that are based on a single reflectance variable. Calibrations including two variables ($trough_{590-730}$, $min_{690or700}$) resulted in a decrease of RMSEP by 15% compared to the best univariate calibration. Including three variables in MLR ($trough_{590-730}$, $min_{690or700}$, min_{480}) resulted in a further decrease of RMSEP by 8%. When including more than three variables, the improvement of the calibration was always <5%. Thus the MLR model including three variables was found to be optimal and was used for the summer temperature reconstruction. The comparison between the instrumental JJAS temperature data and the MLR calibration

Table 5 Comparison of leave-one-out cross-validated RMSEP (°C) for detrended variables

	RMSEP					
	1 variable	2 variables	3 variables	4 variables	5 variables	6 variables
$R_{590}dR_{630}$	0.142					
$R_{570}dR_{630}$	0.136					
$Trough_{590-730}$	0.143					
MLR		Trough; $min_{690or700}$	Trough; $min_{690or700}$; min_{480}	Trough; $min_{690or700}$; min_{480};$R_{570}d_{630}$	All except $min_{690or700}$	All
		0.116	0.102	0.100	0.098	0.098

First the RMSEP of the univariate calibration using inverse regression is shown for the three best variables (correlation with T JJAS $p_{ca} < 0.05$). The RMSEP based on multiple linear regression models including two to six variables shows that including more than three variables does not further improve the calibration model

Fig. 4 Multivariate calibration of detrended 9-year smoothed VIS-RS-derived variables (*blue*) with detrended 9-year smoothed TJJAS (*red*; $r^2 = 0.84$). The calibration model is based on multiple linear regression and includes three variables (Table 5)
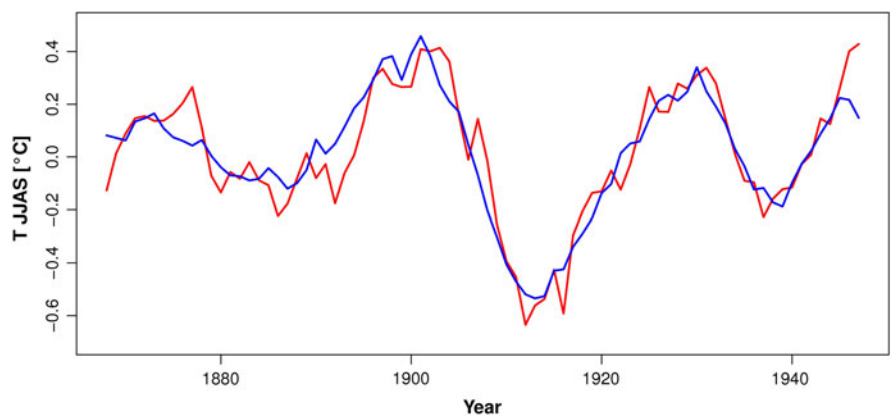
model is shown in Fig. 4 (apparent $r^2 = 0.84$; period 1864–1950: 9-year smoothed, detrended).

Figure 5a and b show the reflectance-based summer temperature reconstruction from Lake Silvaplana back to AD 1177 and the comparison with two independent regional summer temperature reconstructions based on documentary and early instrumental data back to AD 1500 (Casty et al. 2005) and tree-ring data back to AD 1177 (Büntgen et al. 2006).

The 200-year running correlations with the summer (JJA) temperatures of Casty et al. (2005) were significantly positive ($p_c < 0.1$) back to 1715 (time window 1615—1815) and remained positive for the time period back to 1500 (time window 1500–1700; Fig. 5c). The comparison with the tree-ring-based (late-wood density) reconstruction of Büntgen et al. (2006) showed significant ($p_c < 0.1$) positive correlations back to 1760 and between 1480 and 1550 (Fig. 5d).

The decadal-scale variability of summer temperatures is well captured. In particular, extremely cold decades such as the decade AD 1810–1820, with strong negative volcanic forcing are obvious in the reconstruction. The running correlations reveal that, even for longer periods (e.g. AD 1550–1650), the reflectance-based reconstruction performs much better than the tree-ring reconstruction, when compared with the documentary data series. For other periods (e.g. AD 1200, 1450), there is a systematic offset between the lake sediment and the tree-ring time series. This offset is smaller than the dating uncertainties of the age-depth model of the sediment core, and therefore attributable to an imperfect chronology of the lake sediments.

Discussion

Reflectance-derived variables

Four of the six reflectance variables that were extracted from the reflectance spectra are indicative
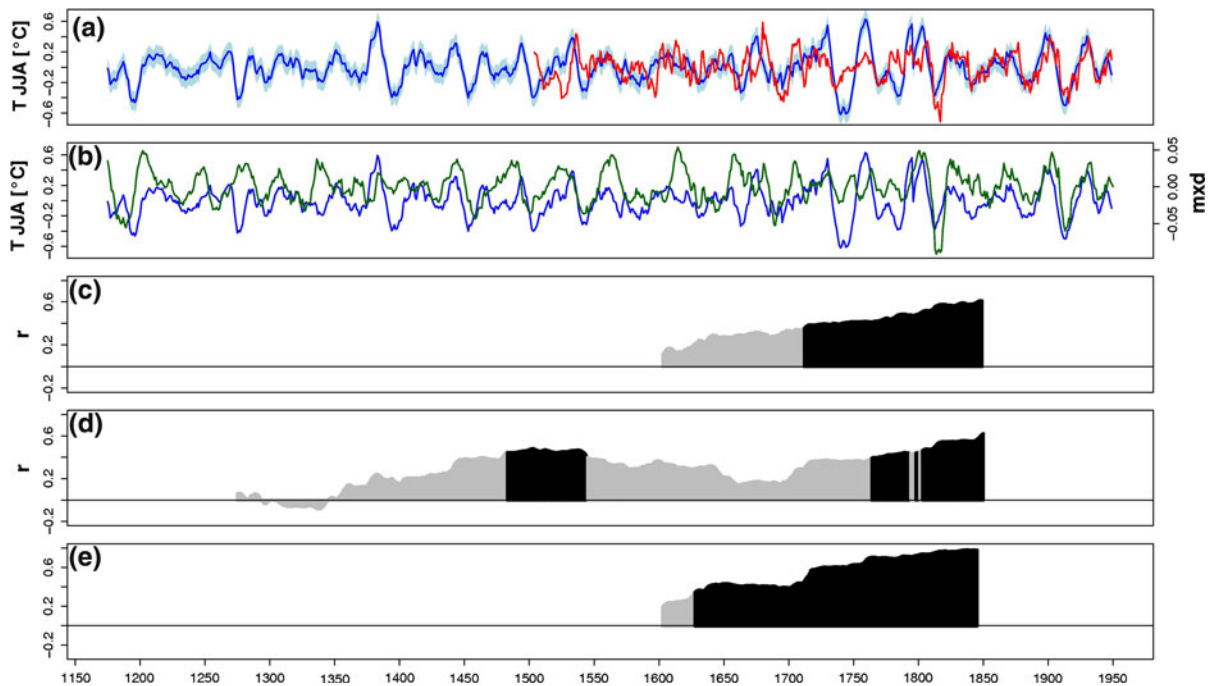
Fig. 5 **a** Comparison of the VIS-RS-inferred T JJAS reconstruction (multiple linear regression including 3 variables, *blue*) with the T JJA reconstruction based on early instrumental and documentary data (*red*; Casty et al. 2005) and with **b** the late-wood density (mxd) based T JJAS reconstruction (*green*; Büntgen et al. 2006). **c** 200-year running correlations between the VIS-RS-inferred T JJAS reconstruction and the T JJA of Casty et al. (2005) and **d** tree-ring based (late-wood density) TJJAS reconstruction (Büntgen et al. 2006). Significant

($p_c < 0.1$) correlations are highlighted in *black*. For running correlation the year indicated is the central year of the 200-year time window. **e** 200-year running correlations between the T JJA reconstruction of Casty et al. (2005) and the TJJAS reconstruction of Büntgen et al. (2006). All data **a** and **b** are 9-year smoothed and LOESS-detrended (span 100 years), thus the reconstruction has skill in the decadal and multi-decadal frequency domains 9–100 year

of the amount of chlorite and mica or combinations of these minerals in the lake sediment (USGS 2007; Rein 2003). A direct quantitative comparison of the variables with XRD measurements (Trachsel et al. 2008) was not possible for two reasons: (1) the XRD was measured in a semi-quantitative way that only allows the calculation of mineral ratios (peak intensity ratio); and (2) the reflectance-derived variables are influenced by the reflectance spectra of several minerals that overlie one another.

The high autocorrelation (lag-1) of five out of six time series is remarkable. This might be interpreted in three ways: (1) due to light scattering on the polyethylene foil and the wet sediment surface, the area integrated in the reflectance measurement might be larger than the aperture of the sensor (diameter = 2.5 mm) to which the light is emitted by the instrument; (2) the variables indicative of illite, biotite and chlorite and min690or700 (unknown)

have high persistence throughout the entire profile and reflect a multi-annual rather than an annual climate signal; (3) the autocorrelation is enhanced by the trend in the time series of the variables $R_{570d}R_{630}$, $R_{590d}R_{690}$ and $min_{690or700}$ (Venables and Ripley 2002). Most likely these three effects interfere with each other and it remains unknown whether the highest possible effective resolution of the VIS-RS data set is as small as the technical resolution (aperture = 2.5 mm) of the instrument.

The autocorrelation in the time series has considerable consequences for the subsequent statistical analyses (correlation and calibration). High autocorrelation decreases the number of independent observations. As a consequence, the degrees of freedom DF need to be adjusted when significance levels are calculated (Trenberth 1984). We recommend rigorous testing and careful assessment of significance levels rather than looking at correlation coefficients *per se*.

PCA reveals large similarities among the first group of variables that describe the slope of the spectra (i.e. between $R_{570}dR_{630}$ and $R_{590}dR_{690}$ [Table 2]). Although the segments are slightly different from each other, they generally reflect the slope of the reflectance spectra between the global maximum, at about 580 nm, and the local minimum at about 690 nm. The variable $R_{570}dR_{630}$ is well established in the literature and reflects the clastic compounds, in particular chlorite, illite or biotite (Rein and Sirocko 2002; Rein 2003). A second group consists of the variables min_{690} and $trough_{590-730}$, both indicative of chlorite (USGS 2007). These variables describe the absorption band depth and the absorption area of the major reflectance minimum at 690 nm. Thus, high similarity between the two variables is expected. The remaining two variables min_{480} and $min_{690or700}$ (Table 1; indication unknown) are different from the other two groups. These variables are poorly or not correlated with climate variables.

Calibration and climate reconstruction

RDA revealed a strong influence of MAR on the reflectance data series. MAR is subject to a low-frequency trend related to glacier length fluctuations (Blass et al. 2007a). To produce a summer temperature reconstruction that is not affected by the trends related to MAR, all variables (predictors and predictands) need to be detrended. RDA for detrended time series is clearly showing that temperature is the main factor influencing the reflectance-derived variables.

Significant correlations between summer temperature and reflectance-derived variables are found for min_{480}, min_{690} and $trough_{590-730}$ for raw (not detrended) 9-year smoothed data and for $R_{570}dR_{630}$, $R_{590}dR_{690}$ and $trough_{590-730}$ for detrended 9-year smoothed data (Table 4). Besides the unknown variable min_{480}, the other significant variables considered here are indicative of chlorite or mica (Rein 2003; USGS 2007). It has been established that, due to the particular geological setting of the catchment (Spillmann 1993), the amount of chlorite and mica is highest in the sediment transported by glacial meltwater (Ohlendorf 1998; Trachsel et al. 2008). During warm summers, glacier meltwater runoff is enhanced and more mica- and chlorite-bearing sediment from the glaciated part of the catchment is transported into the lake.

Considering that this is, to our knowledge, the first methodological attempt to calibrate scanning reflectance (380–730 nm) VIS-RS data from minerogenic lake sediments with meteorological time series, the calibration statistics are remarkable. Individual reflectance variables correlate highly with instrumental summer temperature data during the calibration period AD 1864–1950 ($r > 0.71$ for 5-year smoothed series; $r > 0.82$ for 9-year smoothed series; both highly significant $p_{ca} < 0.05$, p corrected for autocorrelation and multiple testing). The leave-one-out RMSEP of a multivariate calibration model, including the three variables ($trough_{590-730}$, $min_{690or700}$ and min_{480}) is as small as 0.1°C ($r^2 = 0.84$). However, RMSEP is underestimated in autocorrelated time series when calculating leave-one-out RMSEP (e.g. Telford and Birks 2009). Such calibration statistics are rarely found in quantitative paleolimnology and show the great potential of the novel, rapid, non-destructive technique of scanning VIS-RS. It should be noted, however, that the quality of the calibration model and the calibration statistics, i.e. the final product used as a basis for the climate reconstruction, rely critically on an accurate chronology, in this case varve counts, on good knowledge of the mineralogical composition of the individual varves, here determined by XRD, and on a sound understanding of the multiple processes that lead to a specific climate signal in the varves, i.e. meteorology in the catchment, sediment transport and deposition.

The stable significant ($p_c < 0.1$) running correlation with the summer temperatures of Casty et al. (2005) indicates the high stability of the calibration model back in time. The periods with systematic offsets on the order of a few years suggest that the correlation coefficients could be further enhanced by improving the chronology of the sediment core. In this study we left the chronology in its raw form. It is evident, however, that given the high temporal resolution of the data acquired, the accuracy of the chronology is critically important. We recommend that non-destructive scanning reflectance spectroscopy be performed on the same sediment half-core that will later be used to establish the age-depth model by varve counting of thin sections, radioisotopes or other destructive methods.

Conclusions and prospects

We tested the potential of scanning reflectance spectroscopy in the visible spectrum (380–730 nm), measured directly (in situ) on sediment half-cores, to produce quantitative high-resolution (annual–sub-decadal) climate reconstructions from minerogenic lake sediments. For this methodological study, we chose annually laminated deposits from proglacial Lake Silvaplana because the characteristics of the sediments are very well known from previous studies using established analytical techniques. This knowledge allows a sound interpretation of the reflectance spectra measured.

Using MLR, we developed a calibration model that explained 84% of the variance of summer (JJAS) temperature during the calibration period 1864–1950. The correlation of individual variables (indicative of chlorite and mica) were as high as $r = 0.84$. Previous experimental work (XRD) has shown that the amount of chlorite and mica in individual varves is indicative of warm season temperature in Lake Silvaplana.

We used a series of numerical methods and statistical tests to extract a robust climate signal and proper calibration from the multivariate reflectance spectra data set. We first tested the independence of the individual measurements by calculating autocorrelation functions, and then assessed the degree of variance common to the reflectance-derived variables, applying a Principal Component Analysis. We then tested the influence of several potential climate and sediment variables, i.e. temperature, precipitation and MAR, on the reflectance variables by means of Redundancy Analysis. In our case study of Lake Silvaplana we found that the MAR influences the reflectance data. Because MAR in Lake Silvaplana is subject to a low-frequency trend (glacier length variations), we also removed this trend from the reflectance-derived variables prior to calibration to retain a proper temperature signal.

We then tested whether one individual reflectance variable or a combination of variables would yield a better calibration with climate data. Thus, we compared the calibration statistics of systematic univariate and multivariate calibration approaches and found that a calibration model using MLR including three variables performed best. We then applied this calibration model to reconstruct summer temperatures back to AD 1177. This reconstruction was validated by comparing it to two independent regional reconstructions. Running correlation analysis showed high consistency back to at least AD 1600 between all data series. The decadal-scale structure and amplitude of summer temperature variability is well captured. Shorter periods with cold summers, after large tropical volcanic eruptions, are evident, e.g. around AD 1256, 1275, 1450, 1600s and 1810–1820.

We propose the following recommendations for application of in situ scanning reflectance spectroscopy on mineroclastic sediments: (1) non-destructive reflectance spectroscopy should be performed on the same split core that is subsequently used to establish the age-depth model and chronology of the sediment core. This is most critical because high chronological accuracy is fundamental when calibrating the reflectance data set against climate data; (2) prior to interpreting the reflectance spectra, the general mineralogical composition and geochemistry of the sediment should be measured by established analytical methods (e.g. XRD). This provides the basis for a sound interpretation of the reflectance spectra with absorptions of the minerals that are actually present in the sediment.

This study shows the great potential for applying in situ scanning VIS-RS on mineroclastic sediments. From a methodological point of view, the robustness of reflectance characteristics should be further assessed. For instance, it remains unknown to what extent variables such as water content on the split core sediment surface, degree of oxidation of the sediment surface, or temperature influence reflectance measurements. Systematic tests are under way to assess the robustness, reproducibility and technical performance of scanning VIS-RS. However, one key advantage of this method is that it is inexpensive and data are acquired rapidly. Several thousand data points, which correspond to several meters of sediment core, can be generated in one day. This enables systematic study of spatial variability among sediment cores in a given lake (intra-lake variability), which is difficult to achieve with traditional analytical methods. A further avenue of research could involve systematic testing of the method on a variety of lakes with different sediment types and proportions of clastic, biogenic and even chemical components. Although von Gunten et al. (2009) demonstrated the application of the new method on sediments from a

eutrophic lake, with high proportions of organic matter, the method still needs to be tested in a lake with volcanoclastic or chemical sediment (e.g. marl or evaporites), or in lakes with limestone bedrock.

References

Begert M, Schlegel T, Kirchhofer W (2005) Homogeneous temperature and precipitation series of Switzerland from 1864 to 2000. Int J Climatol 25:65–80

Benjamini Y, Hochberg Y (1995) Controlling the false discovery rate: a practical and powerful approach to multiple testing. J R Stat Soc Ser B (Methodological) 57:289–300

Bigler C, von Gunten L, Lotter AF, Hausmann S, Blass A, Ohlendorf C, Sturm M (2007) Quantifying human-induced eutrophication in Swiss mountain lakes since AD 1800 using diatoms. Holocene 17:1141–1154

Birks HJB (1998) Numerical tools in palaeolimnology–Progress, potentialities, and problems. J Paleolimnol 20: 307–332

Blass A, Grosjean M, Troxler A, Sturm M (2007a) How stable are twentieth-century calibration models? A high-resolution summer temperature reconstruction for the eastern Swiss Alps back to AD 1580 derived from proglacial varved sediments. Holocene 17:51–63

Blass A, Bigler C, Grosjean M, Sturm M (2007b) Decadal-scale autumn temperature reconstruction back to AD 1580 inferred from the varved sediments of Lake Silvaplana (southeastern Swiss Alps). Quat Res 68:184–195

Büntgen U, Frank DC, Nievergelt D, Esper J (2006) Summer temperature variations in the European Alps, A.D. 755–2004. J Clim 19:5606–5623

Casty C, Wanner H, Luterbacher J, Esper J, Boehm R (2005) Temperature and precipitation variability in the European Alps since AD 1500. Int J Climatol 25:1855–1880

Caviezel G (2007) Hochwasser und ihre Bewältigung anhand des Beispiels Oberengadin 1750–1900. MSc thesis. University of Bern, Bern

Cleveland WS, Devlin SJ (1988) Locally weighted regression–an approach to regression-analysis by local fitting. J Am Stat Assoc 83:596–610

Dawdy DR, Matalas NC (1964) Statistical and probability analysis of hydrologic data, part III: analysis of variance, covariance and time series. In: Chow VT Handbook of Applied Hydrology, a Compendium of Water-Resources Technology. McGraw-Hill, New York, pp 8.68–8.90

Francus P, Bradley RS, Abbott MB, Patridge W, Keimig F (2002) Paleoclimate studies of minerogenic sediments using annually resolved textural parameters. Geophys Res Lett 29

Frontier S (1976) Etude de la décroissance des valeurs propres dans une analyse en composantes principales: comparaison avec le modèle du bâton brisé. J Exp Mar Biol Ecol 25:67–75

Heegaard E, Birks HJB, Telford RJ (2005) Relationships between calibrated ages and depth in stratigraphical sequences: an estimation procedure by mixed-effect regression. Holocene 15:612–618

Hotelling H (1933) Analysis of a complex of statistical variables into principal components. J Educ Psychol 24(417–441):498–520

Kalugin I, Daryin A, Smolyaninova L, Andreev A, Diekmann B, Khlystov O (2007) 800-yr-long records of annual air temperature and precipitation over southern Siberia inferred from Teletskoye Lake sediments. Quat Res 67:400–410

Kamenik C, Van der Knaap WO, Van Leeuwen JFN, Goslar T (2009) Pollen/climate calibration based on a near-annual peat sequence from the Swiss Alps. J Quat Sci 24: 529–546

Kaufman DS, Schneider DP, McKay NP, Ammann CM, Bradley RS, Briffa KR, Miller GH, Otto-Bliesner BL, Overpeck JT, Vinther BM (2009) Recent warming reverses long-term arctic cooling. Science 325:1236–1239

Legendre P, Legendre L (1998) Numerical ecology. Elsevier, Amsterdam

McKay NP, Kaufman DS, Michelutti N (2008) Biogenic silica concentration as a high-resolution, quantitative temperature proxy at Hallet Lake, south-central Alaska. Geophys Res Lett 35

Michelutti N, Blais JM, Cumming BF, Paterson AM, Ruehland K, Wolfe AP, Smol JP (2009) Do spectrally inferred determinations of chlorophyll a reflect trends in lake trophic status? J Paleolim (online)

Ohlendorf C (1998) High Alpine Lake Sediments as Chronicles for Regional Glacier and Climate History in the Upper Engadine, Southeastern Switzerland. PhD thesis. ETH Zürich, Zürich

Rein B (2003) In situ Reflektionsspektroskopie und digitale Bildanalyse–Gewinnung hochauflösender Paläoumweltdaten mit fernerkundlichen Methoden. Habilitationsschrift. University of Mainz, Mainz

Rein B, Sirocko F (2002) In situ reflectance spectroscopy–analysing techniques for high-resolution pigment logging in sediment cores. Int J Earth Sci 91:950–954

Rein B, Lueckge A, Reinhardt L, Sirocko F, Wolf A, Dullo W (2005) El Nino variability off Peru during the last 20,000 years. Paleoceanography 20: PA 4003

Rosen P, Dodbakk E, Renberg I, Nilsson M, Hall R (2000) Near-infrared spectrometry (NIRS): a new tool for inferring past climatic changes from lake sediments. Holocene 10:161–166

SMA (2002) Jahresbericht der Meteo Schweiz. Annalen der Meteo Schweiz

Spillmann P (1993) Die Geologie des penninischen-ostalpinen Grenzbereichs im südlichen Berninagebirge, PhD thesis. ETH Zürich, Zürich

Telford R, Birks HJB (2009) Evaluation of transfer functions in spatially structured environments. Quat Sci Rev 28: 1309–1316

Trachsel M, Eggenberger U, Grosjean M, Blass A, Sturm M (2008) Mineralogy-based quantitative precipitation,

temperature reconstructions from annually laminated lake sediments (Swiss Alps) since AD 1580. Geophys Res Lett 35:L13707

Trachsel M, Grosjean M, Larocque-Tobler I, Schwikowski M, Blass A, Sturm M (2010) Quantitative summer temperature reconstruction derived from a combined biogenic Si and chironomid record from varved sediments of Lake Silvaplana (south-eastern Swiss Alps) back to AD 1177. Quat Sci Rev 29:2719–2730

Trenberth KE (1984) Some effects of finite sample size and persistence on meteorological statistics. Part I: Autocorrelations. Mon Weather Rev 112:2359–2368

USGS (2007) Digital Spectral Library, splib06a. http://speclab.cr.usgs.gov/spectral-lib.html

van der Wollenberg AL (1977) Redundancy analysis: an alternative for canonical correlation analysis. Psychometrika 42:207–219

Venables WN, Ripley BD (2002) Modern applied statistics with S. Springer, New York

von Gunten L, Grosjean M, Rein B, Urrutia R, Appleby P (2009) A quantitative high-resolution summer temperature reconstruction based on sedimentary pigments from Laguna Aculeo, central Chile, back to AD 850. Holocene 19:873–881

Wolfe AP, Vinebrooke R, Michelutti N, Rivard B, Das B (2006) Experimental calibration of lake-sediment spectral reflectance to chlorophyll a concentrations: methodology and paleolimnological validation. J Paleolimnol 36:91–100

Zolitschka B, Mingram J, van der Gaast S, Jansen JHF, Naumann R (2001) Sediment logging techniques. In: Last WM, Smol JP (eds) Tracking environmental change using lake sediments physical and chemical techniques. Kluwer Academic Publishers, Dordrecht, pp 137–153